Data-based derivation of material response

Adrien Leygue*, Michel Coret, Julien Réthoré, Laurent Stainier, Erwan Verron

GeM - Research Institute of Civil Engineering and Mechanics, UMR 6183, CNRS - Ecole Centrale de Nantes, Université de Nantes, 1, rue de la Noé, 44321 Nantes, France

Abstract

This paper proposes a method to identify the strain–stress relation of non-linear elastic materials, without any underlying constitutive equation. The approach is based on the concept of Data Driven Computational Mechanics recently introduced by Kirchdoerfer and Ortiz (2016). From a collection of non-homogeneous strain fields, for example measured through Digital Image Correlation, the algorithm builds a database of strain–stress couples that sample the mechanical response of the material for the range of measured strains. The method is first derived for truss structures and then extended to the case of small-strain elasticity. The method accuracy, sensitivity to measurement noise and parameters are discussed using manufactured data.
© 2017 Elsevier B.V. All rights reserved.

1. Introduction

Constitutive equations constitute a key concept in mechanical engineering as they relate strain and stress for a given material. The parameters of a constitutive equation are usually adjusted considering a sufficient set of experimental data and appropriate fitting procedures. Beyond the mere description of the mechanical response, a constitutive equation has several purposes:

- it provides a smooth strain–stress relation in which experimental noise has been smeared out,
- for given loading conditions, *e.g.* uniaxial extension, it both interpolates between individual measurements and extrapolates the material response,
- its tensorial nature naturally extends the stress–strain relation to multiaxial loading conditions that are difficult to attain experimentally.

Recently, Kirchdoerfer and Ortiz [1,2] have introduced the concept of Data-Driven Computational Mechanics (DDCM in the following) for elastic materials, in which the constitutive equation vanishes and is replaced by

---

* Corresponding author.
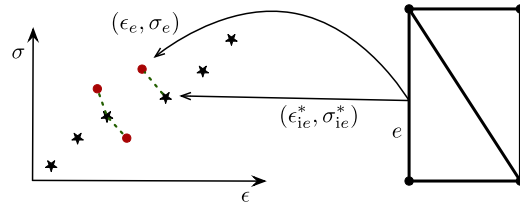 *E-mail address:* adrien.leygue@ec-nantes.fr (A. Leygue).

Fig. 1. The two states (ϵ_e, σ_e) and $(\epsilon_{ie}^*, \sigma_{ie}^*)$ associated to a truss element e. The dashed line represents the energetic mismatch between the two states. On the left we see that the mapping ie between elements and material states can assign the same particular material state to two different elements.

a database of strain–stress couples (called states) which sample the mechanical response of the material. In this approach, regularization/smoothing/interpolation of experimental data are carried out during the computation of the numerical solution of the boundary value problem. The results presented by the authors are encouraging and open the door to many perspectives from the modeling point of view, since the necessity of an explicit or implicit strain–stress relationship is relaxed. In the wake of these contributions, Ibañez et al. [3] investigate the possible use of manifold learning techniques applied to the material database.

Let us briefly recall the method of Kirchdoerfer and Ortiz for data-driven simulation in the particular case of truss structures [1]. It seeks to assign to each truss element e a mechanical state and a material state, a state being a strain–stress couple. Considering both mechanical equilibrium (involving stress) and compatibility conditions (involving strain) as non-questionable, the mechanical state of element e consists of a strain–stress pair (ϵ_e, σ_e) that exactly satisfies the above equations which can be considered as constraints. The second state associated to e, denoted $(\epsilon_{ie}^*, \sigma_{ie}^*)$, is called the material state and is extracted from a collection of admissible material states for the material: $(\epsilon_i^*, \sigma_i^*)$, where $i \in 1 : N^*$. The index i$e \in 1 : N^*$ specifies the material state of element e. It should be interpreted as a pointer that assigns to each element a specific material state in the material database. Fig. 1 illustrates the main ideas behind the method. The proposed solver seeks, for every element simultaneously, a mechanical and a material state as close to each other as possible and such that the former satisfies mechanical equilibrium and compatibility conditions. This is formally expressed as follows:

$$\text{solution} = \arg \min_{\epsilon_e, \sigma_e, \text{i}e} \frac{1}{2} \sum_e w_e \|(\epsilon_e - \epsilon_{ie}^*, \sigma_e - \sigma_{ie}^*)\|_C^2 , \tag{1}$$

subject to

$$\sum_e w_e \mathbf{B}_{ej} \sigma_e = \mathbf{f}_j , \tag{2}$$

and

$$\epsilon_e = \sum_j \mathbf{B}_{ej} \mathbf{u}_j . \tag{3}$$

In the above equations, $\|(\epsilon, \sigma)\|_C$ is an energetic norm, the matrix $\mathbf{B}_{ej}$ encodes the connectivity and geometry of the truss, and w_e denotes the volume of the truss element e. Furthermore, $\mathbf{u}_j$ and $\mathbf{f}_j$ represent, respectively, the displacement and the force applied to truss nodes. For the particular choice

$$\|(\epsilon_e, \sigma_e)\|_C^2 = (C\epsilon_e^2 + \frac{1}{C}\sigma_e^2) , \tag{4}$$

the authors propose an efficient algorithm to solve this problem of combinatorial complexity. The constant parameter (possibly defined element-wise) C is the only parameter of the method and can be interpreted as a modulus associated to the mismatch of mechanical and material states. This mismatch is represented by the dashed lines in Fig. 1.

Although there is no need for a constitutive equation, the database of material states is a mandatory pre-requisite of the method before starting the simulation. Building this database computationally, for example through micro–macro approaches such as FE^2 [4,5], is expensive and might require efficient model order reduction and high dimensional interpolation techniques. From an experimental point of view however it is far from trivial to be able to, somehow,

measure strain and stress over a wide range of strains. Experimentally, except in the case of homogeneous strain/stress configuration, it is not possible to access the stress field. Constitutive law identification from heterogeneous stress field configurations thus relies on inverse parameter identification methodologies. Digital Image Correlation [6] has allowed for significant progress in the field as the result of the numerical simulation of the experiments can be compared to rich data fields (displacement and strain). Such approaches are based on the minimization of a cost function measuring the distance between the numerical and the experimental response. In [7], this cost function is written in terms of strain instead of displacement, because the boundary conditions applied in numerical simulations are usually idealized ones and matching the displacement field may induce artifacts in the identification. An alternative approach is to apply the measured displacement field directly in the numerical simulation. This strategy became a straightforward route as DIC was formulated using finite element shape functions [8]. This allows for measuring displacement fields experimentally with the same kinematic description as for the numerical simulation. Constitutive law parameters identification benefited from this advantage in [9]. In [10], a strategy that is shown to be optimal in terms of noise robustness is elaborated and then developed in [11] for elasto-plastic constitutive laws in combination with 3D finite element simulations. Huang and co-workers [12] have applied the Modified Constitutive Relation Error (M-CRE) introduced by Ladevèze et al. [13] to identify material parameters using a framework that shows some similarity with the starting hypothesis of DDCM: the inviolability of the compatibility and equilibrium equations.

Despite the success of these model-based identification methods, they are all *a priori* constrained by the choice of a constitutive model and are therefore not suited to the DDCM framework. Here we propose a model-free procedure, based on some inversion of the data-driven solver, to extract strain–stress couples that sample the mechanical response of an elastic material. The method uses a collection of displacement and (non homogeneous) strain fields acquired, for example, using Digital Image Correlation techniques. It identifies simultaneously the stress component of the mechanical state for each loading condition and the full material states database, which is common to all loading conditions. The proposed method is first developed for truss structures. The convergence, the influence of measurement noise and parameters are discussed. It is then generalized to a more general small strain elastic problem. In both cases the method is validated considering manufactured data.

2. Data-Driven Identification for truss structures

In this section we propose a method, derived from the data-driven solver of Kirchdoerfer and Ortiz [1], to build the material database by identifying strain–stress couples from experimental measurements.

2.1. Data-Driven Identification (DDI)

Consider a large database of measurements made on real truss structures subject to different loading conditions; all truss elements being of the same material. For each loading condition, or data item, indexed by X, the following quantities are available:

- nodal displacements $\mathbf{u}_j^X$,
- truss geometry and connectivity, encoded through the matrix $\mathbf{B}_{ej}^X$. The mechanical strains are computed as $\epsilon_e^X = \sum_j \mathbf{B}_{ej}^X \mathbf{u}_j^X$,
- applied forces $\mathbf{f}_j^X$,
- prescribed nodal displacements.

Identifying the material response of truss elements reduces to the determination of a finite number N^* of material states $(\epsilon_i^*, \sigma_i^*)$ with $i \in 1 : N^*$, common to all the data items (thus independent of X), and such that

1. for each data item X, the mechanical stress σ_e^X satisfies mechanical equilibrium for X,
2. for each data item X, a material state $(\epsilon_{ie^X}^*, \sigma_{ie^X}^*)$ is assigned to each element e, such that it is close to the mechanical state $(\epsilon_e^X, \sigma_e^X)$ of this element according to a given energetic norm.

It is formulated as follows

$$\text{solution} = \arg \min_{\sigma_e^X, \epsilon_i^*, \sigma_i^*, \mathrm{i}e^X} \mathcal{E}(\sigma_e^X, \epsilon_i^*, \sigma_i^*, \mathrm{i}e^X), \tag{5}$$

with,

$$\mathcal{E}(\sigma_e^X, \epsilon_i^*, \sigma_i^*, ie^X) = \frac{1}{2} \sum_X \sum_e w_e^X \|(\epsilon_e^X - \epsilon_{ie^X}^*, \sigma_e^X - \sigma_{ie^X}^*)\|_C^2 , \tag{6}$$

and subject to

$$\sum_e w_e^X \mathbf{B}_{ej}^X \sigma_e^X = \mathbf{f}_j^X \quad \forall X, j . \tag{7}$$

Unlike the data-driven solver of Kirchdoerfer and Ortiz, the mechanical strain ϵ_e^X is not an unknown of the problem since it can be computed as $\epsilon_e^X = \sum_j \mathbf{B}_{ej}^X \mathbf{u}_j^X$.

At first glance, this problem seems to be quite difficult to solve, but we will show that it can be simplified a great deal. Let us first substitute the expression of the energetic norm Eq. (4) in Eqs. (5)–(6) and introduce a set of Lagrange multipliers η_j^X to enforce the equilibrium constraint Eq. (7). Assuming that the material state mapping ie^X is known, we obtain the following stationarity problem:

$$\delta \left(\sum_X \sum_e \left(\frac{w_e^X C}{2}(\epsilon_e^X - \epsilon_{ie^X}^*)^2 + \frac{w_e^X}{2C}(\sigma_e^X - \sigma_{ie^X}^*)^2 - \sum_j (w_e^X \mathbf{B}_{ej}^X \sigma_e^X - \mathbf{f}_j^X) \cdot \eta_j^X \right) \right) = 0 . \tag{8}$$

Taking all possible variations yields the following set of equations:

$$\delta\epsilon_i^* \Rightarrow \sum_X \sum_{e|ie^X=i} w_e^X C(\epsilon_e^X - \epsilon_{ie^X}^*) = 0 \quad \forall i , \tag{9}$$

$$\delta\sigma_i^* \Rightarrow \sum_X \sum_{e|ie^X=i} w_e^X \frac{1}{C}(\sigma_e^X - \sigma_{ie^X}^*) = 0 \quad \forall i , \tag{10}$$

$$\delta\sigma_e^X \Rightarrow w_e^X \frac{1}{C}(\sigma_e^X - \sigma_{ie^X}^*) - \sum_j w_e^X \mathbf{B}_{ej}^X \eta_j^X = 0 \quad \forall e, X , \tag{11}$$

$$\delta\eta_j^X \Rightarrow \sum_e (w_e^X \mathbf{B}_{ej}^X \sigma_e^X - \mathbf{f}_j^X) = 0 \quad \forall j, X . \tag{12}$$

In the above equations, $\sum_{e|ie^X=i}$ stands for the sum over all elements e such that $ie^X = i$. Eq. (9) simply states that each material strain ϵ_i^* is a weighted average of the mechanical strains in elements assigned to this specific material strain. Similarly Eq. (10) states that each material stress σ_i^* is a weighted average of the mechanical stresses in elements assigned to this specific material stress. The above equations can be simplified and re-interpreted through some simple manipulations. First, the combination of Eqs. (11) and (12) yields

$$\sum_k \sum_e w_e^X C \mathbf{B}_{ej}^X \mathbf{B}_{ek}^X \eta_k^X + \sum_e w_e^X \mathbf{B}_{ej}^X \sigma_{ie^X}^* = \mathbf{f}_j^X \quad \forall j, X. \tag{13}$$

This equation simply states that for any loading case X, the mechanical imbalance between applied forces $\mathbf{f}_j^X$ and material stresses $\sigma_{ie^X}^*$ is balanced by virtual nodal displacements η_j^X considering the pseudo-stiffness C for the truss elements. Second, the combination of Eqs. (10) and (11) yields

$$\sum_{e|ie^X=i} \sum_X \sum_j w_e^X \mathbf{B}_{ej}^X \eta_j^X = 0 \quad \forall i, \tag{14}$$

which merely states that the strains originating from all the virtual displacements η_j^X and associated to a particular material state i have a zero w_e^X-weighted mean. The combination of Eqs. (13) and (14) is a symmetric linear system.

2.2. Solution procedure

To solve the previous set of equations Eqs. (9), (11), (13)–(14) and the material state mapping, we consider the following decoupled algorithm, similar to the one of Kirchdoerfer and Ortiz [1]:

Step 1. Initialize $\mathrm{i}e^X$,
Step 2. compute ϵ_i^* from Eq. (9),
Step 3. simultaneously compute σ_i^* and $\boldsymbol{\eta}_j^X$ from Eqs. (13) and (14),
Step 4. update the value of σ_e^X using Eq. (11),
Step 5. compute a new state mapping $\mathrm{i}e^X$ with

$$\mathrm{i}e^X = \arg\min_{\mathrm{i}e^X} \sum_X \sum_e w_e^X \|(\epsilon_e^X - \epsilon_{\mathrm{i}e^X}^*, \sigma_e^X - \sigma_{\mathrm{i}e^X}^*)\|_C^2 \ , \tag{15}$$

Step 6. iterate Steps 2–5 until convergence of $\mathrm{i}e^X$.

Remarks.

- In Step 1, since the material states are a priori unknown, $\mathrm{i}e^X$ is merely a pointer to an empty value that will be computed later. The initialization provides an initial clustering of the mechanical states that will be improved in Step 5.
  The simplest initialization is to assign to each $\mathrm{i}e^X$ a random integer between 1 and N^*, yielding a random clustering of the mechanical states.
  Since all the mechanical strains ϵ_e^X are known, a very good initialization of $\mathrm{i}e^X$ (or equivalently a clustering of the mechanical states) can be computed through some kmeans-like algorithm [14,15] applied to ϵ_e^X. In this work, we have used the default Matlab® implementation of the Statistics and Machine Learning toolbox.
- Step 2 is relatively inexpensive from a computational point of view as it simply computes the material strains as a weighted average of the mechanical strains.
- Step 3 entails the solution of a large linear system with the following structure:

$$\begin{bmatrix} \mathbf{K}_1 & & & & \mathbf{S}_1 \\ & \mathbf{K}_2 & & & \mathbf{S}_1 \\ & & \ddots & & \vdots \\ & & & \mathbf{K}_{N^X} & \mathbf{S}_{N^X} \\ \mathbf{S}_1^T & \mathbf{S}_2^T & \cdots & \mathbf{S}_{N^X}^T & \mathbf{0} \end{bmatrix} \cdot \begin{bmatrix} \boldsymbol{\eta}_1 \\ \boldsymbol{\eta}_2 \\ \vdots \\ \boldsymbol{\eta}_{N^X} \\ \sigma^* \end{bmatrix} = \begin{bmatrix} \mathbf{f}_1 \\ \mathbf{f}_1 \\ \vdots \\ \mathbf{f}_{N^X} \\ \mathbf{0} \end{bmatrix} ,$$

  where each line corresponds to the assembly of Eq. (13) for a given value of X excepted for the last line which corresponds to the assembly of Eq. (14). All diagonal blocks of the left hand side are constant pseudo-stiffness matrices, while off-diagonal blocks need to be recomputed at each iteration as they depend on $\mathrm{i}e$. This specificity opens the door to efficient resolution schemes that would re-use the initial Cholesky factorization of the diagonal blocks. For example we have observed that an iterative block-Jacobi solver is very efficient.
- Step 4 is computationally inexpensive as it reduces to a matrix vector product.
- In Step 5, to update the state mapping $\mathrm{i}e^X$, we assign to each element e^X the material state that is closest (with respect to $\|\cdot\|_C$). This is relatively expensive as it requires, for each mechanical state, to compute its distance to all material states in the material database. High dimensional generalization of quad-tree algorithms or neighbor lists methods similar to those used in molecular dynamics simulation codes might improve the efficiency of this step.
- Similarly to the data driven solver, the DDI method proposed here entails only few parameters: the number N^* of material states to be identified and the pseudo-stiffness C. It should be noted that C is not necessarily the same for all truss elements and data items, and can therefore depend on both e and X: C_e^X. This provides some additional flexibility in the method and is a tool to weight the data according to some a priori confidence level.
- Even for non-linear material response, the identification procedure only requires the solution of linear systems and simple database searches.
- The success of the proposed method relies on several ingredients. First, the richness of the experimental data over all data items X, *i.e.* the extent of $\mathbf{u}_j^X$ and $\mathbf{f}_j^X$ ensures the identification of the material behavior over a wide range of strains ϵ_i^*. Second the richness of the individual data items, *i.e.* the range of ϵ_i^X for a given X, which couples different material and mechanical states through mechanical equilibrium.
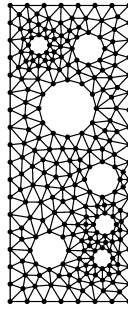
Fig. 2. Undeformed truss structure used for the generation of manufactured data. The structure comprises 249 nodes and 657 nonlinear bar elements.
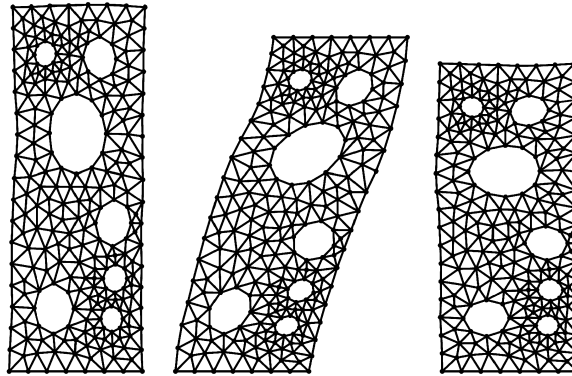

Fig. 3. Three deformed configurations representative of the DDI data-set: traction, shear and compression.

2.3. Numerical results

In this section, the DDI method is applied to the identification of the mechanical response of truss elements exhibiting a non linear strain–stress relation. We use a synthetic dataset generated by applying different loading conditions to the 2D truss structure depicted in Fig. 2. This structure is made of 249 nodes and 657 bar elements with a nonlinear strain–stress behavior of the form: $\sigma = K(\epsilon + \epsilon^3)$, K being set to 5. $N^X = 50$ different loading scenarios involving uniaxial tension and compression, and simple shear have been simulated. Some representative deformed configurations are depicted in Fig. 3. The single parameter C is set to 10 as we do not assume any noise on the mechanical strains ϵ_e^X and therefore wish to put more weight on the strain part of the energetic norm (see Eq. (4)).

Fig. 4 shows, for $N^* = 41$, the computed material and mechanical states together with the "true" constitutive relation used to generate the input data. On top we observe that the $N^* = 41$ identified material states closely match the constitutive relation and that their density is higher for small strains as there are more data points. At the bottom, we observe that all the $N^X \times 657$ mechanical states are distributed close to the material states. The quantization of the material states can be observed through the clustering of the mechanical states around their corresponding material state, for example at large strains or in the inset. Fig. 5 presents, for two different initializations of the state mapping ie, the convergence of the iterative process with respect to the minimized quantity $\mathcal{E}(\sigma_e^X, \epsilon_i^*, \sigma_i^*, ie^X)$. The initialization of ie^X and σ_i^* with a simple kmeans algorithm is so good that the first iteration already outperforms the converged result for a random initialization. All subsequent results are therefore computed with this efficient initialization.

Next, we investigate the influence of noisy input data. Considering that the manufactured data was gathered through Digital Image Correlation with a 1000 by 1000 pixels grid, we add to the displacement fields $\mathbf{u}_j^X$ a zero-mean uniform noise $\delta\mathbf{u}_j^X$ with a one pixel amplitude (hence corresponding to a standard deviation of $\frac{1}{2\sqrt{3}} \approx 0.29$ pixel). This noise model leads to a greater relative influence on small displacements and mechanical strains. It is expected that the addition of noise has the following influence:
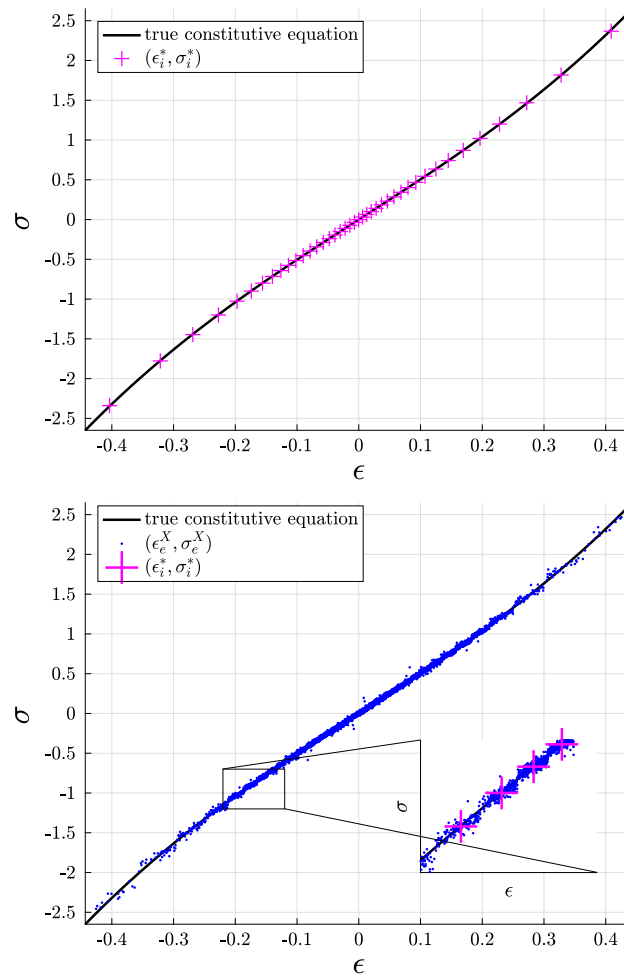
Fig. 4. Material (top) and mechanical (bottom) states computed for $N^* = 41$. There are $N^* = 41$ material states and $N^X \times 657 = 32\,850$ mechanical states. The inset illustrates the clustering of the mechanical states around their assigned material states.
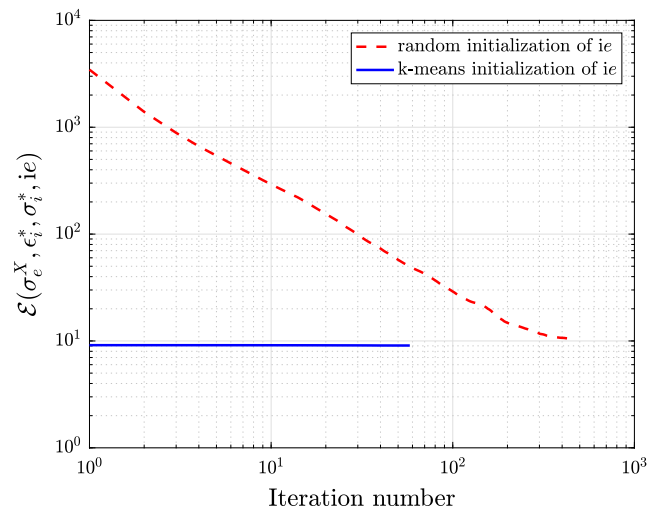

Fig. 5. Comparison of the convergence for two different initializations of ie for $N^* = 41$.
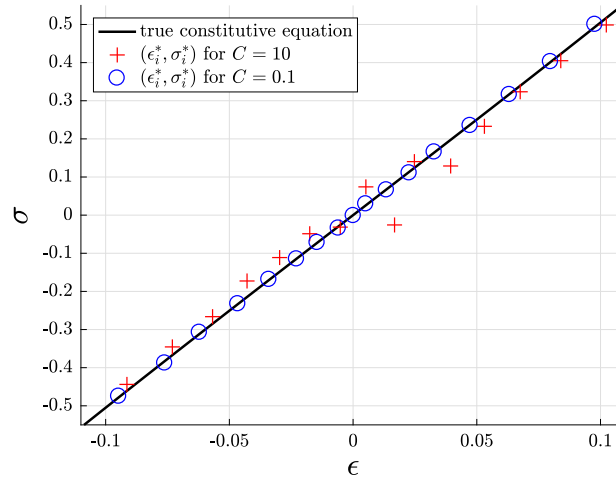
Fig. 6. Influence of C with noisy data.

- If noise does not perturb the state mapping $\mathrm{i}e^X$, it only influences the determination of the material strains ϵ_i^* because Eq. (9) becomes

$$\sum_X \sum_{e|\mathrm{i}e^X=i} w_e^X C(\epsilon_e^X + \delta\epsilon_e^X - \epsilon_{\mathrm{i}e^X}^*) = 0 \quad \forall i.$$

As $\delta\epsilon_e^X = \mathbf{B}_{ej}^X \delta\mathbf{u}_j^X$ has zero mean, it does not introduce any systematic bias in the value of ϵ_i^*. Furthermore, the effect of noisy data is mitigated for large databases of experimental measurements.
- If the amount of noise if sufficient to perturb the state mapping, it also affects the computed values of material σ_i^* and mechanical stress σ_e^X, thereby reducing the quality of results.

In order to mitigate the influence of noisy mechanical strains on the state mapping, we see from Eqs. (4) and (15) that a simple possibility is to reduce the value of C. In Fig. 6 some material states computed for $C = 10$ and $C = 0.1$ are shown. As expected large strain values are less perturbed by noise, and reducing the value of C improves results quality.

3. Data-Driven Identification for elastic materials

In this section we extend the method developed in Section 2 to the more general case of linear elasticity, in the limit of small strains. The major change is that the phase space of material and mechanical states is of much higher dimensionality: a state (mechanical or material) now consists in a linear strain tensor $\boldsymbol{\epsilon}$ and a Cauchy stress tensor $\boldsymbol{\sigma}$, each belonging in a 6-dimensional space (after accounting for their symmetry).

3.1. Data-Driven Identification

Again, we assume the existence of a large database of measurements, obtained by Digital Image Correlation or any related technique. Furthermore we consider a linearized kinematics discretized by a finite element mesh in which each quadrature point e admits an integration weight w_e. For each data item X (or snapshot), the following quantities are available:

- nodal displacements $\mathbf{u}_j^X$,
- finite element geometry and connectivity, encoded through a matrix $\mathbf{B}_{ej}^X$, which compute the mechanical strain $\epsilon_e^X = \sum_j \mathbf{B}_{ej}^X \cdot \mathbf{u}_j^X$,
- applied nodal forces $\mathbf{f}_j^X$,
- prescribed nodal displacements.

The aim of the DDI method is to compute a number N^* of material states $(\boldsymbol{\epsilon}_i^*, \boldsymbol{\sigma}_i^*)$ such that

- for each snapshot X and quadrature point e, it is possible to compute the mechanical state $\boldsymbol{\sigma}_e^X$ that satisfies mechanical equilibrium,
- for each snapshot, a material state $(\boldsymbol{\epsilon}_{ie}^*, \boldsymbol{\sigma}_{ie}^*)$ is assigned to each quadrature point e which is the closest to the mechanical state according to a given energetic norm $\| \cdot \|_{\mathbb{C}}^2$.

Following Kirchdoerfer and Ortiz, we consider

$$\|(\boldsymbol{\epsilon}_e, \boldsymbol{\sigma}_e)\|_{\mathbb{C}}^2 = \frac{1}{2}(\boldsymbol{\epsilon}_e : \mathbb{C} : \boldsymbol{\epsilon}_e + \boldsymbol{\sigma}_e : \mathbb{C}^{-1} : \boldsymbol{\sigma}_e),\tag{16}$$

where $\mathbb{C}$ is a (symmetric positive definite) fourth order stiffness tensor. Like in the truss case, the global minimization problem is

$$\text{solution} = \arg \min_{\boldsymbol{\sigma}_e^X, \boldsymbol{\epsilon}_i^*, \boldsymbol{\sigma}_i^*, ie^X} \mathcal{E}(\boldsymbol{\sigma}_e^X, \boldsymbol{\epsilon}_i^*, \boldsymbol{\sigma}_i^*, ie^X),\tag{17}$$

with

$$\mathcal{E}(\boldsymbol{\sigma}_e^X, \boldsymbol{\epsilon}_i^*, \boldsymbol{\sigma}_i^*, ie^X) = \sum_X \sum_e w_e^X \|(\boldsymbol{\epsilon}_e^X - \boldsymbol{\epsilon}_{ie^X}^*, \boldsymbol{\sigma}_e^X - \boldsymbol{\sigma}_{ie^X}^*)\|_{\mathbb{C}}^2,\tag{18}$$

and subject to the global equilibrium equations:

$$\sum_e w_e^X \mathbf{B}_{ej}^{X\,T} \cdot \boldsymbol{\sigma}_e^X = \mathbf{f}_j^X \quad \forall X, j.\tag{19}$$

All unknowns are real valued except the state mapping ie^X which is discrete. For an arbitrary state mapping, the equilibrium constraints Eq. (19) are enforced by means of Lagrange multipliers $\boldsymbol{\eta}_j^X$, leading to the following problem:

$$\delta \left(\sum_X \sum_e \left(w_e^X (\boldsymbol{\epsilon}_e^X - \boldsymbol{\epsilon}_{ie^X}^*) : \mathbb{C} : (\boldsymbol{\epsilon}_e^X - \boldsymbol{\epsilon}_{ie^X}^*) + w_e^X (\boldsymbol{\sigma}_e^X - \boldsymbol{\sigma}_{ie^X}^*) : \mathbb{C}^{-1} : (\boldsymbol{\sigma}_e^X - \boldsymbol{\sigma}_{ie^X}^*) \right.\right.$$
$$\left.\left. - \sum_j (w_e^X \mathbf{B}_{ej}^{X\,T} \cdot \boldsymbol{\sigma}_e^X - \mathbf{f}_j^X) \cdot \boldsymbol{\eta}_j^X \right) \right) = 0.\tag{20}$$

Taking all possible variations yields the following set of equations:

$$\delta\boldsymbol{\epsilon}_i^* \Rightarrow \sum_X \sum_{e|ie^X=i} w_e^X \mathbb{C} : (\boldsymbol{\epsilon}_e^X - \boldsymbol{\epsilon}_{ie^X}^*) = 0 \quad \forall i\tag{21}$$

$$\delta\boldsymbol{\sigma}_i^* \Rightarrow \sum_X \sum_{e|ie^X=i} w_e^X \mathbb{C}^{-1} : (\boldsymbol{\sigma}_e^X - \boldsymbol{\sigma}_{ie^X}^*) = 0 \quad \forall i\tag{22}$$

$$\delta\boldsymbol{\sigma}_e^X \Rightarrow w_e^X \mathbb{C}^{-1} : (\boldsymbol{\sigma}_e^X - \boldsymbol{\sigma}_{ie^X}^*) - \sum_j w_e^X \mathbf{B}_{ej}^X \cdot \boldsymbol{\eta}_j^X = 0 \quad \forall e, X\tag{23}$$

$$\delta\boldsymbol{\eta}_j^X \Rightarrow \sum_e (w_e^X \mathbf{B}_{ej}^{X\,T} \cdot \boldsymbol{\sigma}_e^X - \mathbf{f}_j^X) = 0 \quad \forall j, X\tag{24}$$

The interpretation of these equations is similar to the interpretation of Eqs. (9)–(12) in Section 2. Combining Eqs. (22), (23) and (24) yields the following linear system, solved to simultaneously determine $\boldsymbol{\sigma}_i^*$ and $\boldsymbol{\sigma}_e^X$ (through $\boldsymbol{\eta}_j^X$):

$$\sum_k \sum_e w_e^X \mathbf{B}_{ej}^{X\,T} : \mathbb{C} : \mathbf{B}_{ek}^X \boldsymbol{\eta}_k^X + \sum_e w_e^X \mathbf{B}_{ej}^{X\,T} \boldsymbol{\sigma}_{ie^X}^* = \mathbf{f}_j^X \quad \forall j, X,\tag{25}$$

and

$$\sum_{e|ie^X=i} \sum_X \sum_j w_e^X \mathbf{B}_{ej}^X \boldsymbol{\eta}_j^X = 0 \quad \forall i.\tag{26}$$

We suggest the following algorithm for computing $\boldsymbol{\epsilon}_i^*$, $\boldsymbol{\sigma}_i^*$, $\boldsymbol{\sigma}_e^X$ and ie:

1. simultaneously initialize $\boldsymbol{\epsilon}_i^*$ and ie by a kmeans algorithm on $\boldsymbol{\epsilon}_e^X$,
2. simultaneously compute $\boldsymbol{\sigma}_i^*$ and $\boldsymbol{\eta}_j^X$ from Eqs. (25)–(26),
3. update the value of $\boldsymbol{\sigma}_e^X$ using Eq. (23),
4. compute a new state mapping ie^X with:

$$\mathrm{i}e^X = \arg\min_{\mathrm{i}e^X} \sum_X \sum_e w_e^X \|(\boldsymbol{\epsilon}_e^X - \boldsymbol{\epsilon}_{\mathrm{i}e^X}^*, \boldsymbol{\sigma}_e^X - \boldsymbol{\sigma}_{\mathrm{i}e^X}^*)\|_{\mathbb{C}}^2 \,, \tag{27}$$

5. update $\boldsymbol{\epsilon}_i^*$ from Eq. (21),
6. iterate steps 2–5 until convergence of ie^X.

Remarks.

- The proposed algorithm is very similar to the one proposed in Section 2, the only difference is the default initialization with the kmeans.
- The most numerically expensive part are steps 2 and 4 which involve the solution of a large linear system and a database search respectively.

3.2. Results and discussion

The method proposed in the previous section is applied to manufactured data. The problem consists in the identification of the mechanical response of a non-linear incompressible material on a bi-dimensional problem, with the plane stress assumption. We consider a 2D finite element mesh with 1340 nodes and 2416 triangular elements, depicted in Fig. 9, and subjected to $N^X = 40$ different loading conditions. Representative deformed configurations are similar to the ones in Fig. 3 in which the bars are now the edges of triangular elements. The constitutive equation used in the FE simulations is of the form:

$$\boldsymbol{\sigma} = G(\boldsymbol{\epsilon} + \alpha\boldsymbol{\epsilon}^3) - p\mathbf{I}\,, \tag{28}$$

$$p = -(\epsilon_{xx} + \epsilon_{yy}) - \alpha(\epsilon_{xx} + \epsilon_{yy})^3\,. \tag{29}$$

where G and α are the material parameters chosen as $G = 5$ and $\alpha = 5$. We consider a tensor $\mathbb{C}$ corresponding to the linearization (i.e. $\alpha = 0$) of the above equation with $G = 1$. In this case, the kmeans initialization of ie^X is so efficient that only a few iterations are necessary to converge for $N^* = 500$.

Since the "true" constitutive equation used to generate the data is isotropic, we first investigate the isotropy of the identified material states. To this end, we compute, for each material state ($\boldsymbol{\epsilon}_i^*$, $\boldsymbol{\sigma}_i^*$), the angle θ_i between the dominant eigenvectors of the strain and stress tensors, respectively. The distribution of these misalignment angles is shown in Fig. 7. We observe that for most of the states, the misalignment angle is less than 1°. This means that the computed material strains and stresses are essentially aligned along the same principal directions, such that the material response can now be examined through the principal strains and stresses. In Fig. 8 we present the first eigenvalue of the material stress tensor (σ_I^*) as a function of the eigenvalues of the corresponding material strain (ϵ_I^*, ϵ_{II}^*). All points fall very close to the surface that can be built from the constitutive equation used to generate the input data:

$$\frac{\sigma_I^*}{G} = \epsilon_I + \alpha\epsilon_I^3 + (\epsilon_I + \epsilon_{II}) + \alpha(\epsilon_I + \epsilon_{II})^3\,. \tag{30}$$

Computed material states therefore provide a discrete description of the "true" material response in the strain range of input data. The observed distribution of material strain in the (ϵ_I^*, ϵ_{II}^*) plane provides an importance sampling of the relevant strain states in the dataset. In particular one can observe the lack data for equibiaxial strain (i.e. $\epsilon_I^* = \epsilon_{II}^*$). The identification of such states might require carefully crafted experiments sampling these states.

We now turn to the analysis of the mechanical stress distributions predicted for all input snapshots. Fig. 9 (top left) presents the predicted von Mises stress for one of the snapshots, and Fig. 9 (top right) shows the relative error. The
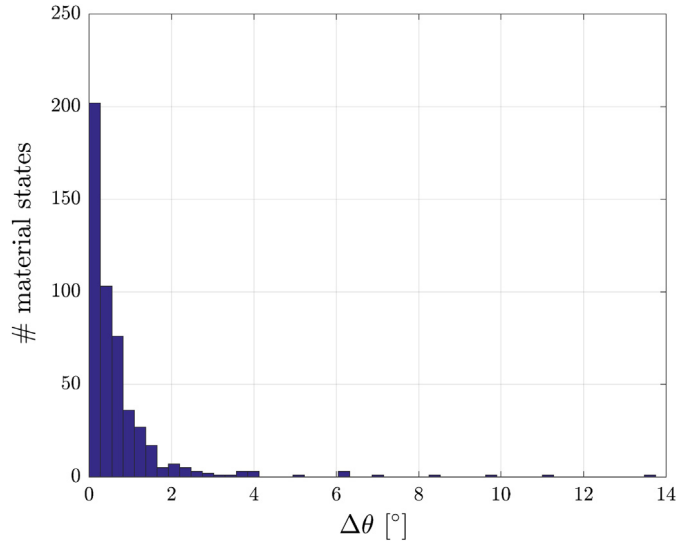
Fig. 7. Distribution of misalignment angle θ between $\boldsymbol{\epsilon}^*$ and $\boldsymbol{\sigma}^*$.
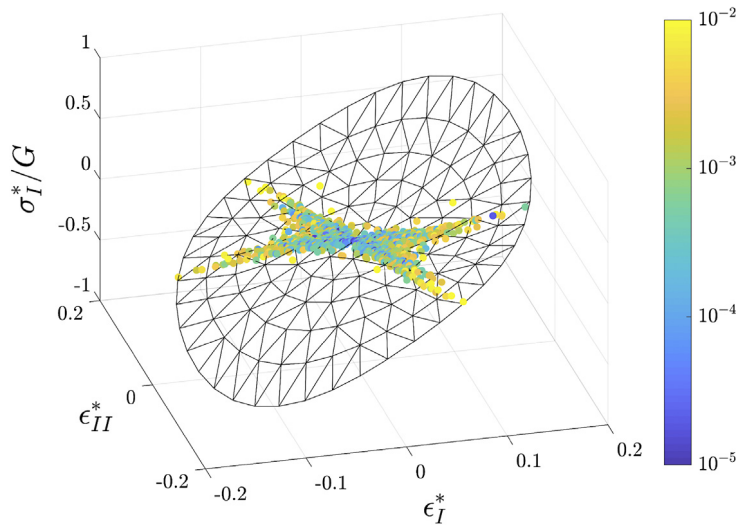

Fig. 8. Largest eigenvalue of the material stress tensor as a function of the eigenvalues of the material strain tensor. The symbols are computed from the identified material states ($\boldsymbol{\epsilon}^*$, $\boldsymbol{\sigma}^*$) and the surface from Eq. (30). The color denotes the vertical distance between the symbols and the analytical surface.

prediction is accurate to less than 10% in most of the domain and reaches 50% in only a few of the 2416 elements, confirming the accuracy of the DDI method. Fig. 9 (bottom) depicts the distribution of the relative error on the von Mises stress for all elements of the 40 snapshots. The observed narrow distribution, with a mean of 8.5% and a median of 5.3% further highlights that the computed mechanical stresses are quite close to the actual ones. Finally, Fig. 10 illustrates the convergence of the identified mechanical stress as a function of the number of material states N^*. We observe a steady convergence of the average error in the von Misses stress over a broad range of N^*. The observed slope is approximately $-\frac{2}{3}$. We also see that a poor initialization lowers the results quality without changing the convergence trend.
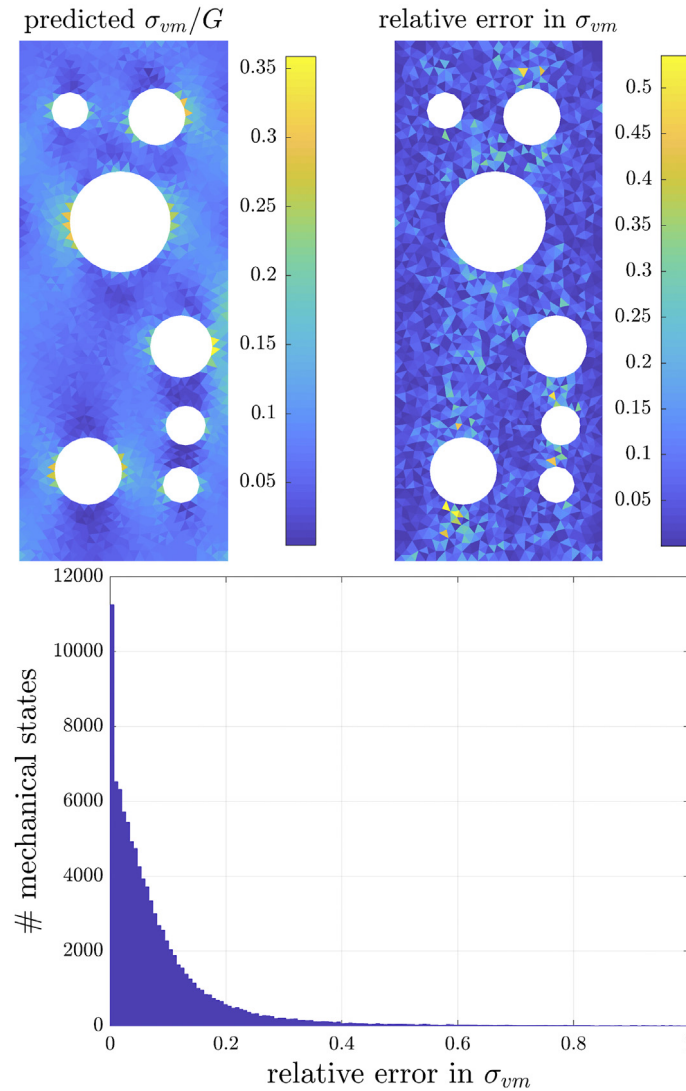
Fig. 9. Top left: predicted von Mises stress field of a particular snapshot computed from the identified mechanical stress. Top right: relative error on the von Mises stress with respect to the true underlying model. Bottom: distribution of the relative error of the von Mises stress for all elements across all snapshots.

4. Summary and concluding remarks

In this paper, we derive a Data Driven Identification (DDI) method that computes admissible strain–stress couples from a set of experimental data, based on the Data-Driven Computational Mechanics (DDCM) framework recently proposed by Kirchdoerfer & Ortiz [1]. The method only requires kinematics and applied forces, which are both accessible using Digital Image Correlation. The computed strain–stress couples can then be used either as constitutive law surrogate in DDCM, or to fit a classical constitutive model. Stress fields of the experimental data are also obtained as a byproduct of the algorithm.

The proposed method is for now applicable to non-linear elastic behaviors only, where stress is uniquely determined by strain. Future developments will focus on more complex material responses such as viscoelasticity, plasticity and damage which involve strain history.
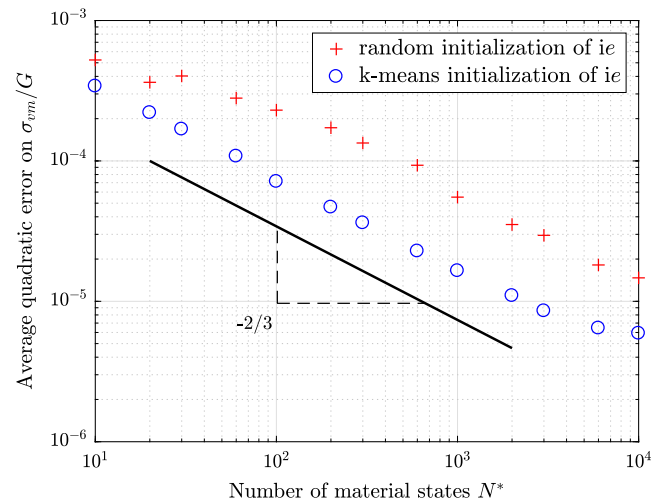
Fig. 10. Convergence, as a function of the number of material states N^*, of the normalized average quadratic error of the von Mises stress for different initializations of the method.

References

[1] T. Kirchdoerfer, M. Ortiz, Data-driven computational mechanics, Comput. Methods Appl. Mech. Engrg. 304 (2016) 81–101.

[2] T. Kirchdoerfer, M. Ortiz, Data driven computing with noisy material data sets, 2017, arXiv:807B8D8C-D147-4234-93C7-2C9FE8B2598A.

[3] R. Ibañez, E. Abisset-Chavanne, J.V. Aguado, D. Gonzalez, E. Cueto, F. Chinesta, A manifold learning approach to data-driven computational elasticity and inelasticity, Arch. Comput. Methods Eng. 46 (15) (2016) 1803.

[4] F. Feyel, Multiscale FE 2 elastoviscoplastic analysis of composite structures, Comput. Mater. Sci. 16 (1–4) (1999) 344–354.

[5] F. Feyel, A multilevel finite element method (FE2) to describe the response of highly non-linear structures using generalized continua, Comput. Methods Appl. Mech. Engrg. 192 (28–30) (2003) 3233–3244.

[6] M.A. Sutton, J.J. Orteu, H. Schreier, Image Correlation for Shape, Motion and Deformation Measurements, in: Basic Concepts, Theory and Applications, Springer Science & Business Media, 2009.

[7] D. Lecompte, A. Smits, H. Sol, J. Vantomme, D. Van Hemelrijck, Mixed numerical–experimental technique for orthotropic parameter identification using biaxial tensile tests on cruciform specimens, Int. J. Solids Struct. 44 (5) (2007) 1643–1656.

[8] G. Besnard, F. Hild, S. Roux, 'Finite-element' displacement fields analysis from digital images: Application to portevin-le châtelier bands, Exp. Mech. 46 (6) (2006) 789–803.

[9] H. Leclerc, J. Perie, S. Roux, F. Hild, Integrated digital image correlation for the identification of mechanical properties, Computer Vision/Computer Graphics CollaborationTechniques, Springer, Berlin, 2009.

[10] J. Réthoré, A fully integrated noise robust strategy for the identification of constitutive laws from digital images, Internat. J. Numer. Methods Engrg. 84 (2010) 631–660.

[11] J. Réthoré, Muhibullah, T. Elguedj, M. Coret, P. Chaudet, A. Combescure, Robust identification of elasto-plastic constitutive law parameters from digital images using 3d kinematics, Int. J. Solids Struct. 50 (1) (2013) 73–85.

[12] S. Huang, P. Feissel, P. Villon, Modified constitutive relation error: An identification framework dealing with the reliability of information, Comput. Methods Appl. Mech. Engrg. 311 (2016) 1–17.

[13] P. Ladeveze, D. Leguillon, Error estimate procedure in the finite element method and applications, SIAM J. Numer. Anal. 20 (3) (1983) 485–509.

[14] J. MacQueen, Some methods for classification and analysis of multivariate observations, University of California Press, 1967, pp. 281–297.

[15] S. Lloyd, Least squares quantization in PCM, IEEE Trans. Inform. Theory 28 (2) (1982) 129–137.